J. Geophys. 45, 373–380, 1979

Journal of Geophysics

Extensions of the Reflectivity Method

R. Kind

Seismologisches Zentralobservatorium, Krankenhausstr. 1–3, D-8520 Erlangen, Federal Republic of Germany

Abstract. The reflectivity method for the computation of theoretical seismograms is extended to include a dislocation point source of arbitrary orientation buried in a layered medium. The second extension is a change in the numerical integration over the circular frequency in order to avoid time aliasing effects.

Key words: Theoretical seismograms – Dislocation point source – Aliasing.

Introduction

The reflectivity method for the computation of theoretical seismograms by Fuchs and Müller (1971) was extended by Kind (1978) to include some types of buried sources, using an analytical development by Harkrider (1964, 1970). The original version by Fuchs and Müller (1971) was extended by Kind and Müller (1975) to include a double couple source. In the following the buried source version will be extended for the case of a buried dislocation point source of arbitrary orientation, using an analytical description of such a source by Harkrider (1976).

In the original version of the reflectivity method the integration over the circular frequency ω was carried out using Fast Fourier Transform methods and equidistant ω spacing. This leads to time aliasing problems for cases in which a seismic phase extends over a longer time duration than the corresponding time window. A solution of this problem is in many cases to increase the length of the time window, but in some cases this is beyond the capacity of the available computer.

The same problem occurs in the wavenumber integration. But this part of the problem was solved by Fuchs (1968). He has carried out the integration over the angle of incidence, instead over the wavenumber k. An equivalent method would be to integrate over the slowness. This change of the variable of integration causes the disappearance of aliasing effects in a certain distance window. Starting from this point, attempts have been made to reduce time aliasing effects as well.

0340-062X/79/0045/0373/$01.60

Displacements and Stresses for a General Source in a Homogeneous Medium

Following Harkrider (1964) we have the following radial and azimuthal dependence for the P-wave potential integrand $\varphi_i(r,\theta,z,k)$ and the S-wave potential integrand $\psi_i(r,\theta,z,k)$ of the source. The index i indicates summation over a number of terms. The symbols for the integration over the wavenumber k are omitted.

$$\begin{aligned}\varphi_i(r,\theta,z,k)&=\varphi_i(z)\,J_i(kr)\,\Lambda_i(\theta)\\ \psi_i(r,\theta,z,k)&=\psi_i(z)\,J_i(kr)\,\Lambda_i(\theta)\end{aligned}\tag{1}$$

where (r,θ,z) is a cylindrical coordinate system, $J_i(kr)$ is the Bessel function of order i, $\varphi_i(z)$ and $\psi_i(z)$ depend on z only and $\Lambda_i(\theta)$ describes the dependence on θ. From the relation between displacement and potential we obtain for the radial and vertical displacement integrand in the farfield

$$\begin{aligned}u_i(r,\theta,z,k)&=\frac{1}{k}\frac{\dot{u}_i}{c}(z)\frac{dJ_i(kr)}{dkr}\Lambda_i(\theta)\\ w_i(r,\theta,z,k)&=-\frac{j}{k}\frac{\dot{w}_i}{c}(z)\,J_i(kr)\,\Lambda_i(\theta)\end{aligned}\tag{2}$$

with

$$\begin{aligned}\frac{\dot{u}_i}{c}(z)&=k^2\left[\varphi_i(z)+\frac{d\psi_i(z)}{dz}\right]\\ \frac{\dot{w}_i}{c}(z)&=jk\left[\frac{d\varphi_i(z)}{dz}+\frac{d^2\psi_i(z)}{dz^2}+k_\beta^2\psi_i(z)\right]\end{aligned}\tag{3}$$

and $k_\beta=\omega/\beta$, where ω is the circular frequency and β the shear velocity, j is the imaginary unit.

Since the source will be described by a discontinuity of the dislocation-stress vector, we also need expressions for the stress P_{zz} normal, and P_{rz} radial tangential to the z-plane. From the relation between stress and potential we obtain

$$\begin{aligned}P_{i_{zz}}(r,\theta,z,k)&=\sigma_i(z)\,J_i(kr)\,\Lambda_i(\theta)\\ P_{i_{rz}}(r,\theta,z,k)&=j\tau_i(z)\frac{dJ_i(kr)}{dr}\Lambda_i(\theta)\end{aligned}\tag{4}$$

with

$$\begin{aligned}\sigma_i(z)&=2\mu\left[\frac{d^2\varphi_i(z)}{dz^2}+\frac{d^3\psi_i(z)}{dz^3}+k_\beta^3\frac{d\psi_i(z)}{dz}\right]-\lambda k_\alpha^2\varphi_i(z)\\ \tau_i(z)&=-jk\mu\left[2\frac{d\varphi_i(z)}{dz}+2\frac{d^2\psi_i(z)}{dz^2}+k_\beta^2\psi_i(z)\right]\end{aligned}\tag{5}$$

where λ and μ are Lame's constants, $k_\alpha=\omega/\alpha$ with the P-velocity α.

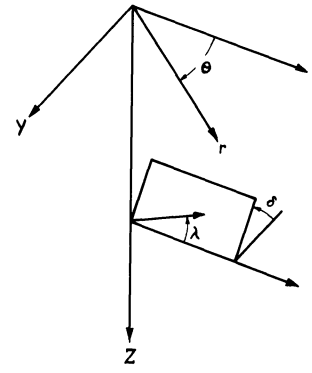

Fig. 1. Geometry of a dislocation source. θ: angle between strike of the fault and observer; δ: dip angle of fault; λ slip direction

The Dislocation Source in a Homogeneous Medium

The geometry of the fault is given in Fig. 1. The *P*- and *S*-wave potentials of this fault, Φ and Ψ, are given by Harkrider (1976) as follows

$$\Phi = \frac{\overline{M}(\omega)}{4\pi\rho\omega^2} \sum_{i=0}^{2} \Lambda_i \int_0^\infty A_i F_\alpha J_i(kr)\, dk$$

$$\Psi = \frac{\overline{M}(\omega)}{4\pi\rho\omega^2} \sum_{i=0}^{2} \Lambda_i \int_0^\infty B_i F_\beta J_i(kr)\, dk \tag{6}$$

with the spectral moment $\overline{M}(\omega)$, the density ρ and

$$\Lambda_0 = \tfrac{1}{2} \sin\lambda \sin 2\delta$$
$$\Lambda_1 = \cos\lambda \cos\delta \cos\theta - \sin\lambda \cos 2\delta \sin\theta$$
$$\Lambda_2 = \tfrac{1}{2} \sin\lambda \sin 2\delta \cos 2\theta + \cos\lambda \sin\delta \sin 2\theta \tag{7}$$

and

$$A_0 = k^2 + 2v_\alpha^2, \quad A_1 = -2\varepsilon k v_\alpha, \quad A_2 = k^2$$
$$B_0 = 3\varepsilon v_\beta, \quad B_1 = (k_\beta^2 - 2k^2)/k, \quad B_2 = \varepsilon v_\beta \tag{8}$$

with $\varepsilon = \text{sign}\,(z-h)$

$$v_v = [k^2 - k_v^2]^{1/2} \qquad k > k_v$$
$$v_v = -j[k_v^2 - k^2]^{1/2} \qquad k < k_v$$

and $v = \alpha, \beta$; source depth h, and

$$F_v = k \exp(-v_v |z-h|)/v_v$$

Comparing (1) and (6) one obtains

$$\varphi_i(z) = \frac{\overline{M}(\omega)}{4\pi\rho\omega^2} A_i F_\alpha$$

$$\psi_i(z) = \frac{\overline{M}(\omega)}{4\pi\rho\omega^2} B_i F_\beta. \tag{9}$$

From (3), (5), and (9) follows

$$\begin{aligned}
\frac{\dot{u}_i^{\pm}}{c}(z) &= Rk^2[A_i k/v_\alpha \mp B_i k] \\
\frac{\dot{w}_i^{\pm}}{c}(z) &= Rjk[\mp A_i k + B_i k^3/v_\beta] \\
\sigma_i^{\pm}(z) &= R[A_i k/v_\alpha(2\mu v_\alpha^2 - \lambda k_\alpha^2) \mp 2\mu B_i k^3] \\
\tau_i^{\pm}(z) &= -Rjk\mu[\mp 2A_i k + B_i k/v_\beta(k^2 + v_\beta^2)]
\end{aligned} \tag{10}$$

with $R = \overline{M}(\omega)/(4\pi\rho\omega^2)$.

The plus and minus sign indicate $z > h$ and $z < h$, respectively. The exponential term is omitted in (10).

Denoting $(\Delta_{i_1}, \Delta_{i_2}, \Delta_{i_3}, \Delta_{i_4})$ the discontinuity of the displacement-stress vector at $z = h$, then we have

$$\begin{pmatrix} \Delta i_1 \\ \Delta i_2 \\ \Delta i_3 \\ \Delta i_4 \end{pmatrix} = \begin{pmatrix} \dot{u}_i/c(z)^+ \\ \dot{w}_i/c(z)^+ \\ \sigma_i(z)^+ \\ \tau_i(z)^+ \end{pmatrix} - \begin{pmatrix} \dot{u}_i/c(z)^- \\ \dot{w}_i/c(z)^- \\ \sigma_i(z)^- \\ \tau_i(z)^- \end{pmatrix} \tag{11}$$

from (11), (10), and (8) follows for $i = o$

$$\begin{pmatrix} \Delta_{0_1} \\ \Delta_{0_2} \\ \Delta_{0_3} \\ \Delta_{0_4} \end{pmatrix} = \begin{pmatrix} 0 \\ 4Rjk^2k_\alpha^2 \\ 0 \\ 2Rjk_\mu^2(3k_\beta^2 - 4k_\alpha^2) \end{pmatrix} \tag{12}$$

for $i = 1$

$$\begin{pmatrix} \Delta_{1_1} \\ \Delta_{1_2} \\ \Delta_{1_3} \\ \Delta_{1_4} \end{pmatrix} = \begin{pmatrix} -Rk^2k_\beta^2 \\ 0 \\ 0 \\ 0 \end{pmatrix} \tag{13}$$

and for $i = 2$

$$\begin{pmatrix} \Delta_{2_1} \\ \Delta_{2_2} \\ \Delta_{2_3} \\ \Delta_{2_4} \end{pmatrix} = \begin{pmatrix} 0 \\ 0 \\ 0 \\ 2Rjk^2\mu k_\beta^2 \end{pmatrix} \tag{14}$$

Displacements at the Free Surface Due to a Dislocation Source Buried in a Layered Medium

The Fourier transformed displacement components are obtained from (2)

$$\bar{u}(r,\theta,z) = \int_0^\infty \frac{1}{k} \sum_{i=0}^{2} \frac{\dot{u}_i}{c}(z) \frac{dJ_i(kr)}{dkr} \Lambda_i(\theta)\, dk$$

$$\bar{w}(r,\theta,z) = -\int_0^\infty \frac{j}{k} \sum_{i=0}^{2} \frac{\dot{w}_i}{c}(z)\, J_i(kr)\, \Lambda_i(\theta)\, dk. \tag{15}$$

In order to obtain the displacements at the free surface, we replace in (15) the displacement integrands at the depth z in the full space by $\dot{u}_i/c(0)$ and $\dot{w}_i/c(0)$ at the free surface with the source buried in the layered medium. The displacement integrands at the free surface are obtained from

$$R_{11}\frac{\dot{u}_i}{c}(0) = (R^h_{11} R^h_{12} R^h_{13} R^h_{15} R^h_{16}) \begin{pmatrix} -A_{22} & A_{12} & 0 & 0 \\ -A_{32} & 0 & A_{12} & 0 \\ -A_{42} & -A_{32} & A_{22} & A_{12} \\ 0 & -A_{42} & 0 & A_{22} \\ 0 & 0 & -A_{42} & A_{32} \end{pmatrix} \begin{pmatrix} \Delta_{i_1} \\ \Delta_{i_2} \\ \Delta_{i_3} \\ \Delta_{i_4} \end{pmatrix}$$

$$-R_{11}\frac{\dot{w}_i}{c}(0) = (R^h_{11} R^h_{12} R^h_{13} R^h_{15} R^h_{16}) \begin{pmatrix} -A_{21} & A_{11} & 0 & 0 \\ -A_{31} & 0 & A_{11} & 0 \\ -A_{41} & -A_{31} & A_{21} & A_{11} \\ 0 & -A_{41} & 0 & A_{21} \\ 0 & 0 & -A_{41} & A_{31} \end{pmatrix} \begin{pmatrix} \Delta_{i_1} \\ \Delta_{i_2} \\ \Delta_{i_3} \\ \Delta_{i_4} \end{pmatrix} \tag{16}$$

Equation (16) are due to Kind (1978). The R^h_{st} are Dunkin's (1965) delta matrix elements of the J matrix, where J is the product Haskell matrix of the halfspace and all layers up to the source. R_{11} is the Rayleigh function of the complete model. The matrix A is the product of the Haskell layer matrices above the source. From (15) one obtains in time domain, applying (16)

$$u(r,\theta,t) = \int_{-\infty}^{+\infty} \int_0^\infty \frac{K_u(w,k)}{k} \exp(-j(kr-\omega t))\, dk\, d\omega$$

$$w(r,\theta,t) = \int_{-\infty}^{+\infty} \int_0^\infty \frac{-jK_w(\omega,k)}{k} \exp(-j(kr-wt))\, dk\, dw \tag{17}$$

with

$$K_u(\omega,k) = \frac{\exp(\pi/4)}{\sqrt{2\pi \mathrm{kr}}} \left[-j\Lambda_0(\theta)\frac{\dot{u}_0}{c}(0) + \Lambda_1(\theta)\frac{\dot{u}_1}{c}(0) + j\Lambda_2(\theta)\frac{\dot{u}_2}{c}(0) \right]$$

$$K_w(\omega,k) = \frac{\exp(\pi/4)}{\sqrt{2\pi kr}} \left[\Lambda_0(\theta)\frac{\dot{w}_0}{c}(0) + j\Lambda_1(\theta)\frac{\dot{w}_1}{c}(0) - \Lambda_2(\theta)\frac{\dot{w}_2}{c}(0) \right]$$

where the asymptotic approximation of the Bessel functions for large arguments in positive direction of propagation is used. Equation (17) may be considered as a double Fourier-transformation from the (ω, k)-domain to the (r, t)-domain.

The Numerical Integration

The numerical integration of (17) seems simple. Fast Fourier Transform programs could be applied successively for the integration over k and ω. The

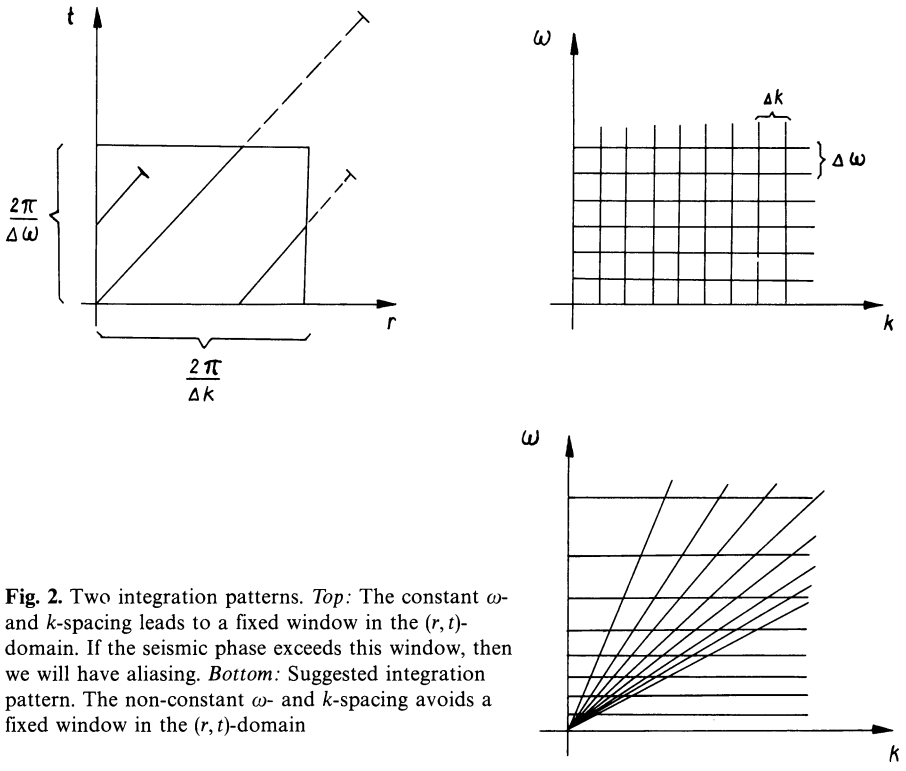

Fig. 2. Two integration patterns. *Top:* The constant ω- and k-spacing leads to a fixed window in the (r,t)-domain. If the seismic phase exceeds this window, then we will have aliasing. *Bottom:* Suggested integration pattern. The non-constant ω- and k-spacing avoids a fixed window in the (r,t)-domain

integrand could be set zero for $k<0$. The spacing in the (ω,k)-domain determines the window in the (r,t)-domain, and the Nyquist (ω,k)-values determine the spacing in the (r,t)-domain. However, this works only if aliasing problems can be disregarded. This is illustrated in Fig. 2. If the spacing in the (ω,k)-domain is not close enough, so that a seismic phase reaches the boundaries of the according window in the (r,t)-domain, then we will have aliasing. Fuchs (1968) has introduced a method to avoid aliasing in the distance domain. He has carried out the integration over the angle of incidence intead over k. This subdivides the (ω,k)-domain in a manner, which is shown in the lower part of Fig. 2. There it may be seen, that the k-spacing is not longer constant. On the other hand, Fuchs (1968) was still using a constant ω-spacing.

The general problem is, how the (ω,k)-plane may be sampled in order to reduce aliasing effects in the (r,t)-plane. A very similar problem appears in the design of arrays (Haubrich, 1968). There one is searching the best pattern for a fixed number of instruments in the two dimensional r-domain, in order to minimize aliasing (side lobes) in the two dimensional k-domain. Aliasing effects are reduced in this case by using nonequal spacing. This method is adopted for the present problem. A disadvantage of this integration method over non-equidistant intervals is however, that Fast Fourier methods cannot be used any more in the usual way. One from many possible patterns for the non-constant ω-spacing is indicated in the lower part of Fig. 2. We have for small frequencies a small ω-

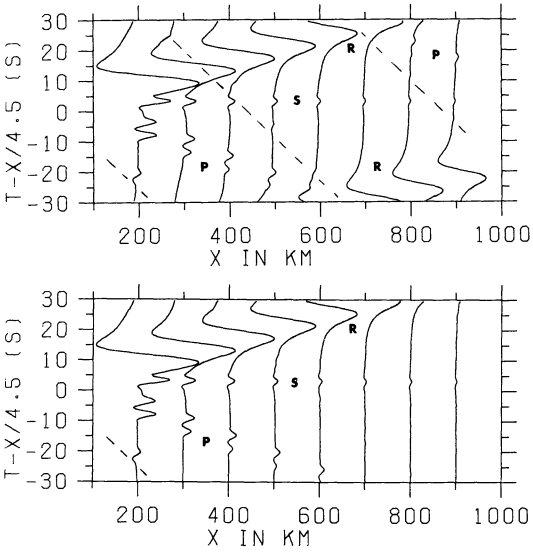

Fig. 3. Theoretical seismograms for two different ω-integration methods: *Top:* constant ω-spacing. *Bottom:* Variable ω-spacing. The source is a single vertical force at 30 km depth in a halfspace. The *dashed line* indicates a numerical phase connected with the limit of the k-integration. All phases due to aliasing have disappeared in the bottom case. R: Rayleigh wave; P: P-wave; S: S-wave

spacing (or a large time window), and for large frequencies a large ω-spacing (or a small time window). Such a pattern may be obtained using the following recursive equation:

$$\omega_{i+1} = \omega_i + 2\pi / \left[T + a \cdot 2\pi / \left(\omega_i + \frac{2\pi}{T} \right) \right] \quad \text{for } i = 0 \ldots n \tag{18}$$

with the starting value $\omega_0 = 0$, when T is the desired duration of the seismogram, and with $a > 0$. The first non-zero ω-value is $\omega_1 = 2\pi/(T + a \cdot T)$, for high frequencies approaches the ω-increment $2\pi/T$. The value ω_n is the desired largest circular frequency.

An example of the new ω-integration is shown in Fig. 3. The horizontal radial component is shown in this figure, observed at the free surface due to a single vertical force at 30 km depth in a homogeneous halfspace. The P-velocity in the halfspace is 6 km/s and the S-velocity is 4.5 km/s. Numerical examples of multilayered models and dislocation point sources may be found in Kind (1978; 1979). The results of the integration with a constant ω-spacing is shown on top of the figure. The Rayleigh wave and the P-wave reach the boundaries of the time window and are continued at the other side o the time window. At the bottom of Fig. 3 are shown the same seismograms for an ω-integration with non-constant ω-spacing. The value a in (18) was 4.5. All phases caused by aliasing have disappeared. The integration time only, was about eight times larger in the bottom case, about 50 % more frequencies have been computed. It must be kept in mind, that the integration time is only a small percentage of the total computer time, if the model consists of many layers. More computer time can be saved if more storage is available. In practical cases the disadvantage of the longer computer time may be reduced because of the possibility to compute

now very short time windows only. The variable ω-spacing integration was carried out using the trapezoidal rule.

Conclusions

The extension of the reflectivity method for a buried dislocation point source allows now to interpret farfield earthquake records. The changed ω-integration makes it now possible to compute only short time windows, even if the seismogram has a very long duration.

Acknowledgement. This research was supported by the Deutsche Forschungsgemeinschaft. I wish to thank Gerhard Müller for reading the manuscript and Paul Richards for discussions.

References

Dunkin, J.W.: Computation of modal solution in layered media at high frequencies. Bull. Seismol. Soc. Am. **55**, 335–358, 1965

Fuchs, K.: The reflection of spherical waves from transition zones with arbitrary depth-dependent elastic moduli and density. J. Phys. Earth **16** (Special Issue), 27–41, 1968

Fuchs, K., Müller, G.: Computation of synthetic seismograms with the reflectivity method and Comparison with observations. Geophys. J. R. Astron. Soc. **23**, 417–433, 1971

Harkrider, D.G.: Surface waves in multilayered elastic media, 1. Rayleigh and love waves from buried sources in a multilayered elastic half space. Bull. Seismol. Soc. Am. **54**, 627–679, 1964

Harkrider, D.G.: Surface waves in multilayered elastic media, Part II. Higher modes spectra and spectral ratios from point sources in plane layered earth models. Bull. Seismol. Soc. Am. **60**, 1937–1987, 1970

Harkrider, D.G.: Potentials and displacements from two theoretical seismic sources. Geophys. J. R. Astron. Soc. **47**, 97–133, 1976

Haubrich, R.A.: Array design. Bull. Seismol. Soc. Am. **58**, 977–991, 1968

Kind, R., Müller, G.: Computation of SV waves in realistic earthmodels. J. Geophys. **41**, 149–172, 1975

Kind, R.: The reflectivity method for a buried source. J. Geophys. **44**, 603–612, 1978

Kind, R.: Observations of sPn from Swabian Alb earthquakes at the GRF Array. J. Geophys. (in press, 1979)

Received February 8, 1979; Revised Version May 29, 1979; Accepted May 29, 1979